

The crystal structure of Ba(Ce_{0.8}Zr_{0.2})O₃

Jong Sung Bae^{a,*}, Woong Kil Choo^a, Chang Hee Lee^b

^aDepartment of Materials Science and Engineering, Korea Advanced Institute of Science and Technology, 373-1 Gusong-Dong, Yusong-Gu, Taejeon, South Korea

^bNeutron Physics Department, HANARO Center, Korea Atomic Energy Research Institute, Taejeon 305-600, South Korea

Received 4 September 2000; received in revised form 2 November 2000; accepted 15 November 2000

Abstract

The crystal structure of perovskite based Ba(Ce_{0.8}Zr_{0.2})O₃ has been determined by X-ray and neutron powder diffractions. The space group has been established by Rietveld refinement. Our final analysis indicates that the space group of Ba(Ce_{0.8}Zr_{0.2})O₃ is Imma with an anti-phase oxygen octahedral tilting along the two crystallographic axes. At a temperature above the transition, 1273 K, the high temperature prototype phase is found to be cubic $Pm\bar{3}m$. © 2001 Elsevier Science Ltd.

Keywords: Crystal structure; Fuel cells; Perovskites; X-ray methods

1. Introduction

Trivalent rare earth-doped BaCeO₃ has been investigated extensively due to its high ionic conduction property for electrolyte in solid oxide fuel cell (SOFC) application.^{1,2} However, its application has been restricted to oxygen atmosphere, instead of reformer gas under ambient atmosphere, because its chemical stability deteriorates on contact with CO₂ and H₂O.³ Recent studies have reported that the chemical stability can be increased by zirconium substitution, in spite of the unavoidable reduction in ionic mobility.⁴ But, 20% Zr substitution is considered to be enough for the structural stability, not sacrificing conductivity too much.⁵

The crystal structure of BaCeO₃ is reported to be orthorhombic at room temperature with the space group *Incn* and transited to *F32/n*, and then finally to $Pm\bar{3}m$ with the increase in temperature.⁶ However, there is a contradicting report that its room temperature structure is *Pnma* then it transforms to cubic $Pm\bar{3}m$ at high temperature via intermediate *Imma* and $R\bar{3}C$ phase.⁷

A raman study suggested that phase transition occurs also in Zr substituted BaCeO₃,⁸ but there are no structural studies by neutron and X-ray diffractometry to support such a claim.

The purpose of this work is to investigate the crystal structure of 20% Zr substituted BaCeO₃ which is

reported to be structurally stable and which may provide the fundamental information about ionic transport phenomena.^{9,10}

2. Experimental

Ba(Ce_{0.8}Zr_{0.2})O₃ was synthesized by solid state reaction from the mixed BaCO₃, CeO₂ and ZrO₂ powders at 1400°C for 7 h. X-ray powder diffraction patterns were collected at room temperature on a Rigaku Rotaflex diffractometer using CuK_α radiation equipped with a graphite monochromator [$\lambda = 1.5418 \text{ \AA}$, $2\theta = 20\text{--}130^\circ$]. The neutron powder diffraction pattern was collected at room temperature and at 1273 K on a high-resolution powder diffractometer (HRPD) [$\lambda = 1.8430 \text{ \AA}$, $2\theta = 20\text{--}130^\circ$] at the Hanaro reactor, Korea Atomic Energy Research Institute. Test powders were compacted in a vanadium cylinder and were heated in vacuum. Neutron beams from the reactor were monochromated by the Ge(331) single crystal. The structure refinement was carried out on a FULLPROF program (LLB-France) which adopts the Rietveld calculation method.

3. Results and discussion

Figs. 1 and 2 are the X-ray and neutron diffraction profiles of Ba(Ce_{0.8}Zr_{0.2})O₃ at room temperature. A rather simple pattern implying a high symmetry is observed. In addition to the fundamental reflections,

* Corresponding author. Tel.: +82-42-869-4253; fax: +82-42-869-4273.

E-mail address: coyote07@cais.kaist.ac.kr (J.S. Bae).

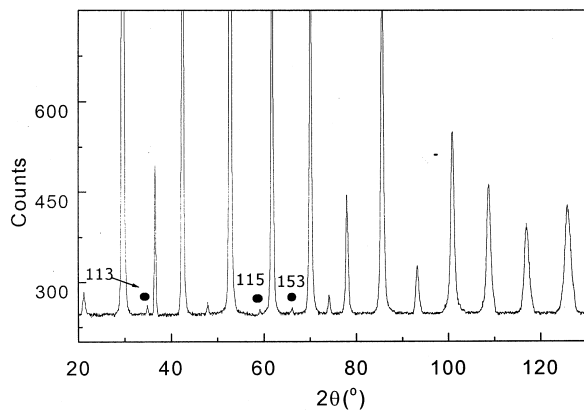


Fig. 1. Room temperature X-ray diffraction pattern of $\text{Ba}(\text{Ce}_{0.8}\text{Zr}_{0.2})\text{O}_3$; filled circles represent $\{h+1, k+1, l+1\}_p$ type superlattice reflections.

extra diffraction lines are shown. X-ray superlattice lines appear more conspicuously at low angles and their relative intensity is much lower. This means that these extra peaks arise due to either the oxygen octahedral tilting or the cation modulation. A direct evidence that the superlattice lines are attributed to tilting is that the neutron relative intensity of these lines is much stronger than that of the X-ray because the neutron oxygen scattering cross section is significant in comparison with the cation cross sections. For convenience, we chose the doubled unit cell of a perovskite cell in considering the inphase and antiphase tilting. In order to determine the space group, the mode of oxygen octahedral tilting should be determined correctly. The superlattice lines are indexed in reference to the doubled perovskite prototype unit cell of which basis vectors may be converted from that of the orthorhombic unit cell, satisfying the following vector relationships.

$$a_p = -a_o + c_o, b_p = a_o + c_o, c_p = b_o. \quad (1)$$

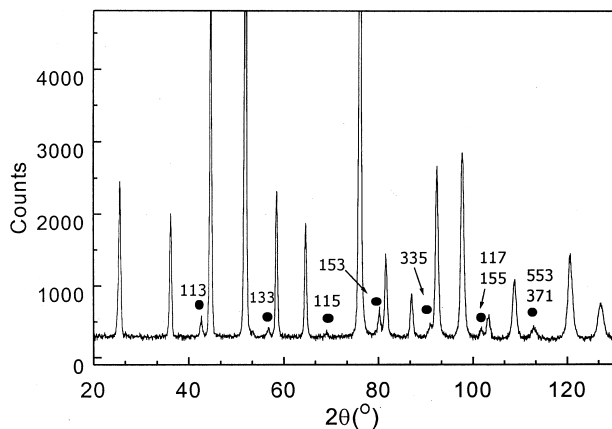


Fig. 2. Room temperature neutron diffraction pattern of $\text{Ba}(\text{Ce}_{0.8}\text{Zr}_{0.2})\text{O}_3$; filled circles represent the octahedral tilting superlattice reflections.

Only the odd-odd-odd ($h \neq 1$) type indices were identified. No even or mixed indices are found. According to the Glazer¹¹ and Woodward,¹² the tilting mode which satisfies the above conditions is $a^-b^-b^-$ and the space group is determined to $Imma$ (#74). The indexing result in reference to the prototype structure obeys the reflection condition very well.

The objective of this study is two fold. Firstly, we set out to determine the crystal structure of $\text{Ba}(\text{Ce}_{0.8}\text{Zr}_{0.2})\text{O}_3$, which has been determined to be $Imma$. Secondly, we wanted to know whether $\text{Ba}(\text{Ce}_{0.8}\text{Zr}_{0.2})\text{O}_3$ goes through a phase transition. To find out the second objective, we conducted neutron scattering at room temperature and at 1273 K.

To confirm the space group $Imma$, Rietveld refinement has been executed. The calculated fitting profile is superposed in Fig. 3. The fitted curves and observed patterns are in the solid lines and the circle markers respectively. The vertical marks in the middle represent the calculated Bragg positions. The traces in the bottom plots are the difference between the calculated and observed intensities. The atomic positions are changed from the positions in the aristotype perovskite phase. Antiphase tiltings along the two axes and non-tilting along the remaining axis were assumed. Schematic projections are drawn in Fig. 4 from the refined data. The final atomic coordinates are listed in Table 1.

In order to find out the high temperature crystal structure, refinements on the neutron data were also carried out at 1273 K, Fig. 5. We can clearly see that all the superlattice lines have disappeared. Hence, the crystal structure of the high temperature prototype phase is cubic $Pm\bar{3}m$. Our numerical results indicate that the calculated fit is a satisfactory one. We have not been able to determine the transition temperature in this study, but we have established that $\text{Ba}(\text{Ce}_{0.8}\text{Zr}_{0.2})\text{O}_3$ undergoes a phase transition somewhere in between room temperature and 1273 K.

In studying perovskites stability, the Goldschmidt tolerance factor is very helpful. It is defined by

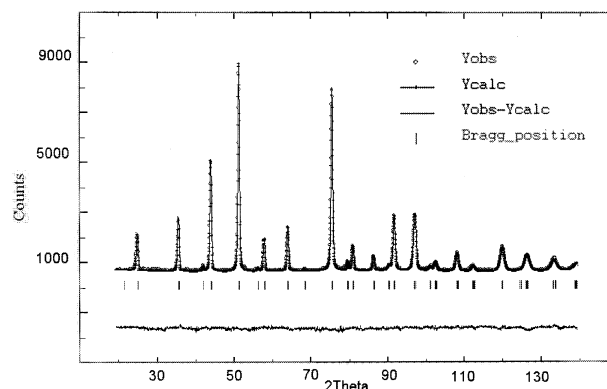


Fig. 3. Powder neutron diffraction pattern fittings for $\text{Ba}(\text{Ce}_{0.8}\text{Zr}_{0.2})\text{O}_3$ at room temperature in space group $Imma$.

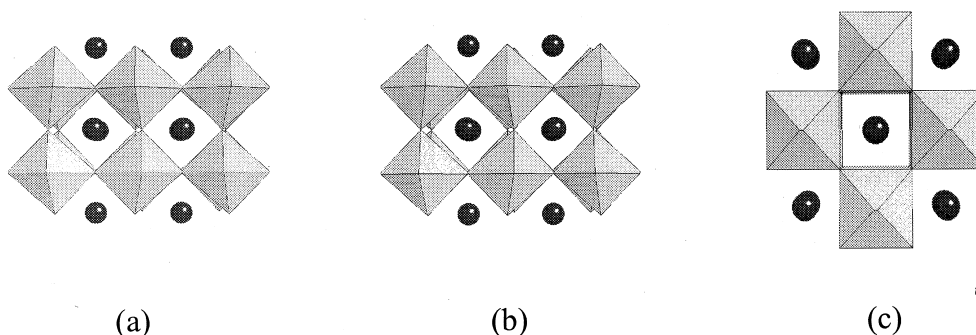


Fig. 4. Schematic projection of the crystal $\text{Ba}(\text{Ce}_{0.8}\text{Zr}_{0.2})\text{O}_3$ structure on the plane normal to the octahedral along the (a) $[100]_p$, (b) $[010]_p$ and (c) $[001]_p$ prototype axes.

Table 1
Refined fractional atomic coordinates and displacement parameters at (a) room temperature and (b) at 1273 K

	<i>x</i>	<i>y</i>	<i>z</i>	<i>B</i>
(a)				
Ba	0	0.25	0.02129	0.83143
Ce	0	0	0.5	0.38394
Zr	0	0	0.5	0.88
O1	0.5	0.25	−0.0113	0.96707
O2	0.25	−0.01969	0.75	0.29867
$R_{wp} = 1.57$	$R_{Bragg} = 0.8$	$a = 5.9805$	$b = 8.4794$	$c = 6.0019$
(b)				
Ba	0.5	0.5	0.5	0.73794
Ce	0	0	0	0.43348
Zr	0	0	0	0.60952
O	0	0.5	0.5	0.10470
$R_{wp} = 2.12$	$R_{Bragg} = 1.18$	$a = 4.2716$	$b = 4.2716$	$c = 4.2716$

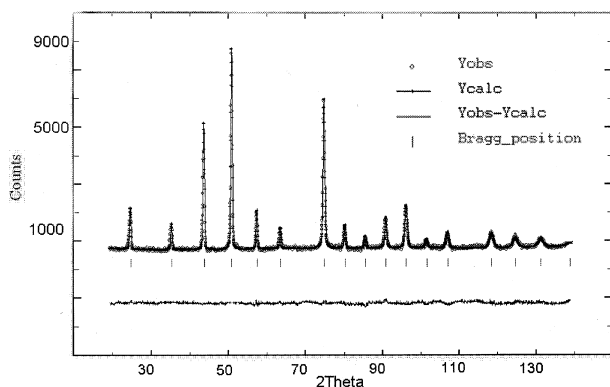


Fig. 5. Powder neutron diffraction pattern fittings for $\text{Ba}(\text{Ce}_{0.8}\text{Zr}_{0.2})\text{O}_3$ at 1273 K in space group $Pm\bar{3}m$.

$$t = \frac{r_A + r_O}{\sqrt{2}(r_B + r_O)} \quad (2)$$

where r_A , r_B and r_O are the radii of the A and B cations and oxygen ion respectively. The more deviated is the tolerance factor from unity, the more distorted is the

structure. When the space generated by the oxygen octahedra is close packed by cations, an ideal cubic phase is fully established, while larger B-site cations tend to cause the oxygen atoms to induce oxygen octahedral tilting.^{13,14} In calculating the tolerance factor, the ionic radii data were taken from Muller and Roy.¹⁵ In $\text{Ba}(\text{Ce}_{0.8}\text{Zr}_{0.2})\text{O}_3$, its tolerance factor is increased from 0.96674 to 1.0035 by substituting smaller Zr^{4+} [$R^{IV} = 0.86 \text{ \AA}$] for Ce^{4+} [$R^{IV} = 0.94 \text{ \AA}$]. Hence, the number of the $\text{Ba}(\text{Ce}_{0.8}\text{Zr}_{0.2})\text{O}_3$ $a^+a^-a^-$ tilting axes is reduced to two from three of the BaCeO_3 $a^+a^-a^-$ tilting. Yet, we notice that the ionic size difference is not as large as to induce a B-site ordering.

4. Conclusion

The crystal structure of $\text{Ba}(\text{Ce}_{0.8}\text{Zr}_{0.2})\text{O}_3$ has been determined to be orthorhombic, space group $Imma$, at room temperature. However, at 1273 K the positions of oxygen atoms become more symmetric due to the thermal motion. As a consequence, $Pm\bar{3}m$ cubic space group appears at the high temperature most solid oxide fuel cells are operated.

Acknowledgements

This research was achieved by the support of nuclear basic research program 1999' in Korea. The authors deeply appreciate the support.

References

- Wienstroer, S. and Wiemhofer, H. D., Investigation of the influence of zirconium substitution on the properties of neodymium-doped barium cerates. *Solid State Ionics*, 1997, **101**, 1113–1117.
- Chen, F. L., Toft S-orensen, Meng, G. Y. and Peng, D. K., Preparation of Nd-doped BaCeO_3 proton conducting ceramic and its electrical properties in different atmospheres. *J. Eur. Ceram. Soc.*, 1998, 1389.
- Scholten, M. J. and Schoonman, J., Synthesis of strontium and

- barium cerate and their reaction with carbon dioxide. *Solid State Ionics*, 1993, **61**, 83–91.
4. Kreuer, K. D., On the development of proton conducting materials for technological applications. *Solid State Ionics*, 1997, **97**, 1.
 5. Ryu, K. H. and Haile, S. M., Chemical stability and proton conductivity of doped $\text{BaCeO}_3\text{--BaZrO}_3$. *Solid State Ionics*, 1999, **125**, 355–367.
 6. Knight, K. S., Structural phase transition in BaCeO_3 . *Solid State Ionics*, 1994, **74**, 109–117.
 7. Genet, F., Loridant, S., Ritter, C. and Lucazeau, G., Phase transition in BaCeO_3 : neutron diffraction and raman studies. *J. Phys. Chem. Sol.*, 1999, **60**, 2009–2021.
 8. Charrier-Cougoulic, I., Pagnier, T. and Lucazeau, G., Raman spectroscopy of perovskite-type $\text{BaCe}_x\text{Zr}_{1-x}\text{O}_3$ ($0 \leq x \leq 1$). *J. Phys. Chem. Sol.*, 1999, **142**, 220–227.
 9. Glockner, R., Islam, M. S. and Norby, T., Proton and other defects in BaCeO_3 : a computational study. *Solid State Ionics*, 1999, **122**, 145–156.
 10. Knight, K. S., Powder neutron diffraction studies of $\text{BaCe}_{0.9}\text{Y}_{0.1}\text{O}_{2.95}$ and BaCeO_3 at 4.2 K: a possible structural site for the proton. *Solid State Ionics*, 2000, **127**, 43–48.
 11. Glazer, A. M., The classification of tilted octahedra in perovskites. *Acta Cryst.*, 1972, **B28**, 3384.
 12. Woodward, M., Octahedral tilting in perovskites I. Geometrical consideration. *Acta Crystall.*, 1997, **B53**, 32–43.
 13. Thomas, N. W., Crystal structure–physical property relationships in perovskites. *Acta Crystall.*, 1989, **B45**, 337.
 14. Thomas, N. W., The compositional dependence of octahedral tilting in orthorhombic and tetragonal perovskites. *Acta Crystall.*, 1996, **B52**, 16.
 15. Muller, O. and Roy, R., *The Major Tendency Structural Families*. Springer-Verlag, Berlin, 1974 (pp. 5).